Interlaminar Shear Strength for Three Kinds of Ceramic Matrix Composites at 1173K

Jianjie GOU, Chengyu ZHANG, Shengru QIAO, Xuanwei WANG

National key Laboratory of Thermostructure Composite Materials, Northwestern Polytechnical University, Xi'an 710072, P. R. China

blao@nwpu.edu.cn

Abstract: Interlaminar shear strength (ILSS) of a two-dimensional carbon fiber reinforced silicon carbide (2D-C/SiC) composite, two-and-a-half-dimensional carbon fiber-reinforced silicon carbide (2.5D-C/SiC) composite along the warp and weft directions and two-dimensional silicon carbide fiber reinforced silicon carbide (2D-SiC/SiC) composite were investigated by the double-notch shear (DNS) test at 1173K in air. The microstructure and fracture morphologies of the DNS specimens were observed by a scanning electron microscope (SEM) and an optical microscope. Experimental data shows that ILSS of 2.5D-C/SiC along the warp direction is not only lower than that of the weft direction, but also lower than 2D-C/SiC. Besides, ILSS for 2D-SiC/SiC is higher than that of the 2D-C/SiC. The possible reasons are analyzed through SEM images, optical micrographs and results of ILSS at 1173K in air. Finally the fracture mechanism is discussed.

Key words：Ceramic matrix composites; ILSS; Fracture morphology

1. Introduction

Successful development of Continuous Fiber-reinforced Ceramic Matrix Composites (CFCCs) has led to great improvements to the intrinsic problems of brittleness, low fracture toughness and catastrophic failure of the monolithic ceramic. CFCCs are now used in various high-temperature applications, such as structural materials for aerospace industry, aircraft brakes, burner nozzles and rocket thrusters [1-3]. However, even though CFCCs have shown significant increase of damage tolerance and the ability of resistance to fracture in in-plane area, inherent processing defects or cracks in the matrix-rich interlaminar regions of the CFCCs can cause delamination under shear stress, resulting in some kind of structural failure [4-6].

A number of studies with respect to the shear properties for CFCCs have been reported. In-plane and interlaminar shear strength of a unidirectional SiC fiber-reinforced $(BaSr)Al_2Si_2O_8$ celsian composite were measured by the double-notch shear (DNS) test method between room temperature and 1473K, the difference in layer architecture and alignment of fiber-rich layers with the shear plane in the interlaminar specimens appeared to be the reason for the lower strength of this composite [7]. Choi et al investigated the interlaminar mechanical properties determined for six

different CFCCs at ambient temperature and observed the degradation of interlaminar shear strength (ILSS) with decreasing shear stress rate, containing SiC fiber-reinforced SiC matrix composites, SiC fiber-reinforced glass ceramic composites and carbon fiber-reinforced SiC matrix composites [8,9]. Investigation of the life limiting behavior of the melt-infiltrated Hi-Nic SiC/SiC subjected to interlaminar shear was made at 1589K in air under stress rupture loading [10]. M.B. Ruggles-Wrenn and P.D. Laffey investigated the creep behavior of the Nextel™720/alumina (N720/A) composite in interlaminar shear loading at 1473K in air environments [11]. In our previous work, ILSS of 2D-C/SiC at elevated temperature was investigated in air [12]. Nevertheless, a comparison of several kinds of ceramic matrix composites on ILSS in the same condition is still very limited up to now, especially at elevated temperature. Since 2D-C/SiC, 2.5D-C/SiC and 2D-SiC/SiC are commonly used at high temperature, so a detailed investigation and comparison of the shear properties of these composites at elevated temperature appears to be necessary.

The objective of this work was to compare the shear behaviors of 2D-C/SiC, 2.5D-C/SiC and 2D-SiC/SiC. Double-notch shear (DNS) test method was specified to determine ILSS of ceramic matrix composites at elevated temperature by American Society for Testing and Materials (ASTM) standard (C-1425-05) [13]. ILSS of the mentioned ceramic matrix composites was determined by DNS at 1173K in air. An analysis of material damage and the failure characteristics with respect to different fibers and woven structures was discussed in the text.

2. Experimental

2.1 Materials and Specimens

The 2D-C/SiC,2.5D-C/SiC and 2D-SiC/SiC composites used in this study were fabricated by chemical vapor infiltration (CVI) of SiC into preforms. Fibrous preforms for 2D-C/SiC and 2D-SiC/SiC are plain weaving structure, while fibrous preform for 2.5D-C/SiC is shown in Fig.1. The fibers were coated with pyrocarbon (PyC) with thickness of 200 nm before infiltration of SiC matrix. Residual porosity is sealed by depositing on the external surface of the specimens a suitable coating at the end of the process.　The parameters of tested composites are listed in table 1.
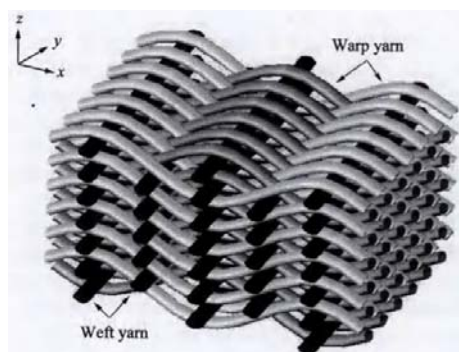

Figure 1. Schematic diagram of fiber perform for 2.5D-C/SiC composite

Table 1. The parameters of tested composites

materials	reinforcement	preforms	fiber volume fractions (%)	Bulk density (g/cm^3)	residual porosity(%)
2D-C/SiC	3K-PAN carbon fibers	2D	40	1.99	15
2.5D-C/SiC	3K-PAN carbon fibers	2.5D	45	2.05	15
2D-SiC/SiC	0.25K silicon carbide fibers	2D	40	2.61	11.5 (open porosity)

Interlaminar shear failure was conducted in a region between two notches that were asymmetrically located on opposite sides of the specimens at an equal distance from the mid-plane, as shown in Fig.2. A layer of SiC coating was deposited on the specimens after the machining of notches, and the thickness of coating was added to specimen dimension. It's worth noting that both the warp loading direction and weft loading direction of the specimens for 2.5D-C/SiC were fabricated respectively.
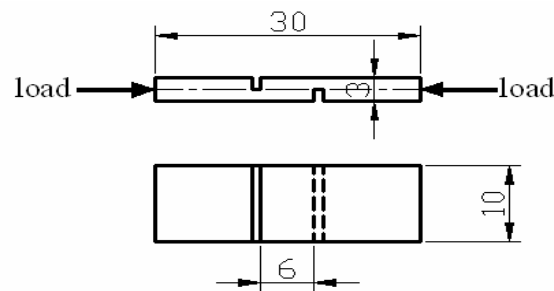

Figure 2.Geometry and dimensions of the DNS specimen

2.2 Mechanical property measurement

All tests were performed at 1173K in air. The specimens were heated at a rate of 40–50K/min, followed by a soaking period of 10 min after reaching the test temperature. Then the DNS specimens were applied to a compression load along the specimen axis, as shown in Fig. 2. Monotonic loading was carried out in displacement control at a rate of 0.595 mm/min. Five specimens were tested for each kind of ceramic matrix composites. The ILSS is calculated as Eq. 1:

$$ILSS = P_{max}/WL \tag{1}$$

Where P_{max} is the ultimate compressive load, W is the specimen width and L is the notch spacing between the inner franks of the notches.

The morphologies of fracture surfaces were examined by a scanning electron microscope (SEM, HITACHI S-4700) and an optical microscope.

3. Results and discussion

3.1 Shear load versus cross-head displacement curves

Fig. 3 displays the shear load versus cross-head displacement curves obtained at 1173K in air. In the initial loading stage, nonlinearity exists for all curves. Except the curve of 2.5D-C/SiC along the warp direction, the slopes of curves keep increasing until to peak load followed by a sudden load drop when the specimens failed, although the test was conducted under a constant rate of 0.595 mm/min. It suggests that the process containing a stable propagation of cracks in the interlaminar region is impossible, and that shear failure occurs whenever the inherent ILSS is reached partly anywhere in the shear plane.
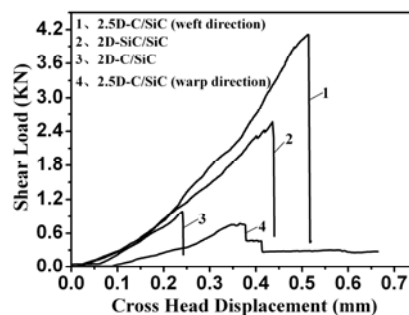

Figure 3. Interlaminar shear load versus cross-head displacement curves from
the compression of DNS specimens for the three kinds of ceramic matrix

It can be found for the curve of 2.5D-C/SiC along the warp direction that the stage prior to failure is similar to those mentioned above, while several steps occur after reaching the peak load, which is related to the special weaving structure.

3.2 ILSS at 1173K

ILSS of the tested specimens at 1173K in air are shown in Fig. 4. It clearly shows that ILSS of 2D-C/SiC is higher than that of 2.5D-C/SiC along the warp direction，but considerably lower compared with that of the weft direction for 2.5D-C/SiC. The great shear anisotropy between the warp and weft direction for 2.5D-C/SiC can be understood by the characteristics of the fiber preform architecture, shown in Fig.1. When the specimens were subjected to a shear load along the

weft direction, the load was mainly carried by weft yarns and then by the weft and contacted warp yarns. What's more, being interlocked by tightly contacted warp yarns, the lateral movements of the weft yarns were well restricted. Conversely, in the warp direction, the fewer distributed weft yarns couldn't perfectly limit the lateral movements of warp yarns, and the sinusoidal warp yarns may weaken the ability of resistance to failure.
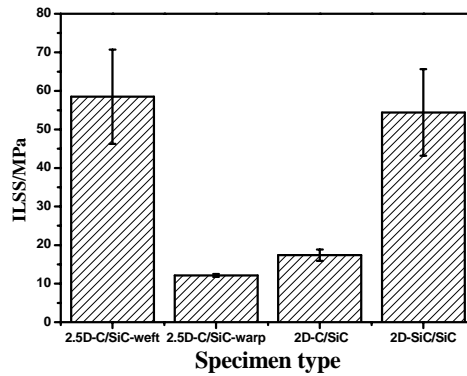

Figure 4. ILSS of the three kinds of composites at 1173K in air

ILSS for 2D-SiC/SiC is considerably higher than that of the 2D-C/SiC. The poor ILSS for 2D-C/SiC is mainly associated with the oxidation of fibers. This will be discussed further from the SEM observations.

3.3 Fracture morphology

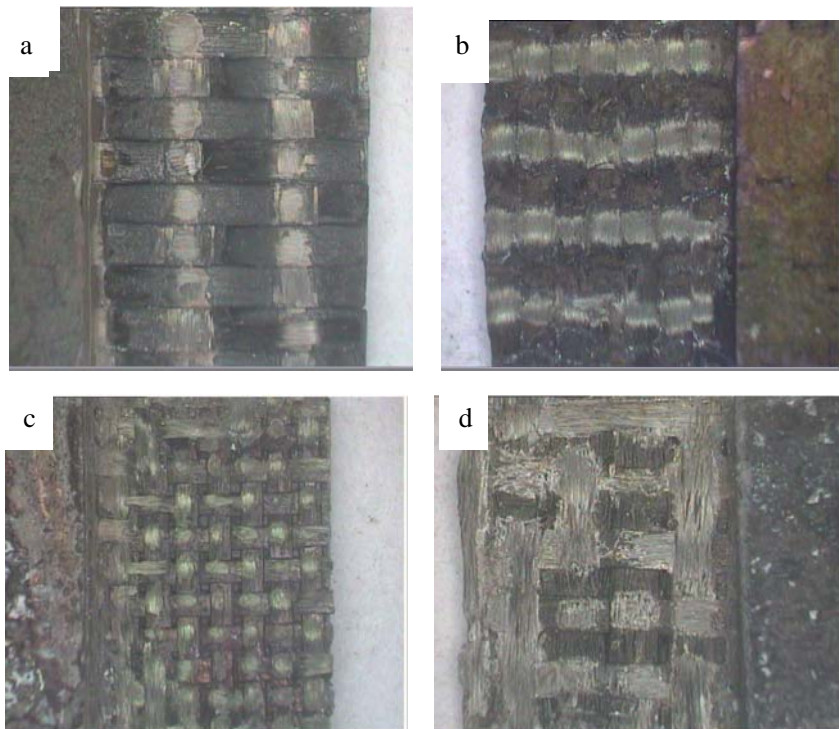Fig. 5 presents typical optical micrographs of fracture surface for the three kinds of composites.

Figure 5. Optical micrographs of the failed 2.5D-C/SiC along the warp (a) and weft (b)
direction, 2D-C/SiC (c)and 2D-SiC/SiC (d) specimens.

All the specimens failed in a typical shear mode along their respective interlaminar shear planes. As shown in Fig. 5(a) and (b) for 2.5D-C/SiC, it can also prove that only the fewer weft interlocked yarns played a resisting role in the process of shear failure along the warp direction，while the more interlocked yarns resist to fracture and fracture surface is rough in the weft direction.

As presented in Fig. 5(c) and (d), for 2D-C/SiC and 2D-SiC/SiC, the fracture surfaces are both somewhat smooth and clean, and the fiber bundle are clearly observed.

Owing to a mismatch of the thermal expansion coefficients of the fibers and matrix, a certain mount of microcracks already exist in the SiC coating as well as in the SiC matrix upon cooling from the processing temperature for the three kinds of composites. And microcracks are formed in the coating that favor the in-depth diffusion of oxygen. When shear test is carried out at 1173K, the oxygen can diffuse through these microcracks and reach to the carbon interface and fibers. The oxidation kinetics is controlled by the gas-phase diffusion through the microcracks in the SiC coating, resulting in a nonuniform degradation of the carbon phases [15]. The oxidation of carbon interface and fiber causes degradation of bond between the fiber and matrix, so the fiber is easier pulling out owing to the weak interface, as illustrated in Fig. 6(a). Due to the inhomogeneous SiC coating and stress concentration in the vicinity of notches, failure of the specimens usually generates from the notches, resulting in severe oxidation at this site (Fig. 6(b)). Carbon fibers are rapidly oxidized at temperatures above 400°C, while the silicon carbide fiber possesses relatively high anti-oxidation temperature, as shown in Fig. 6(c) and (d), consequently, ILSS of 2D-SiC/SiC is higher than that of 2D-C/SiC.
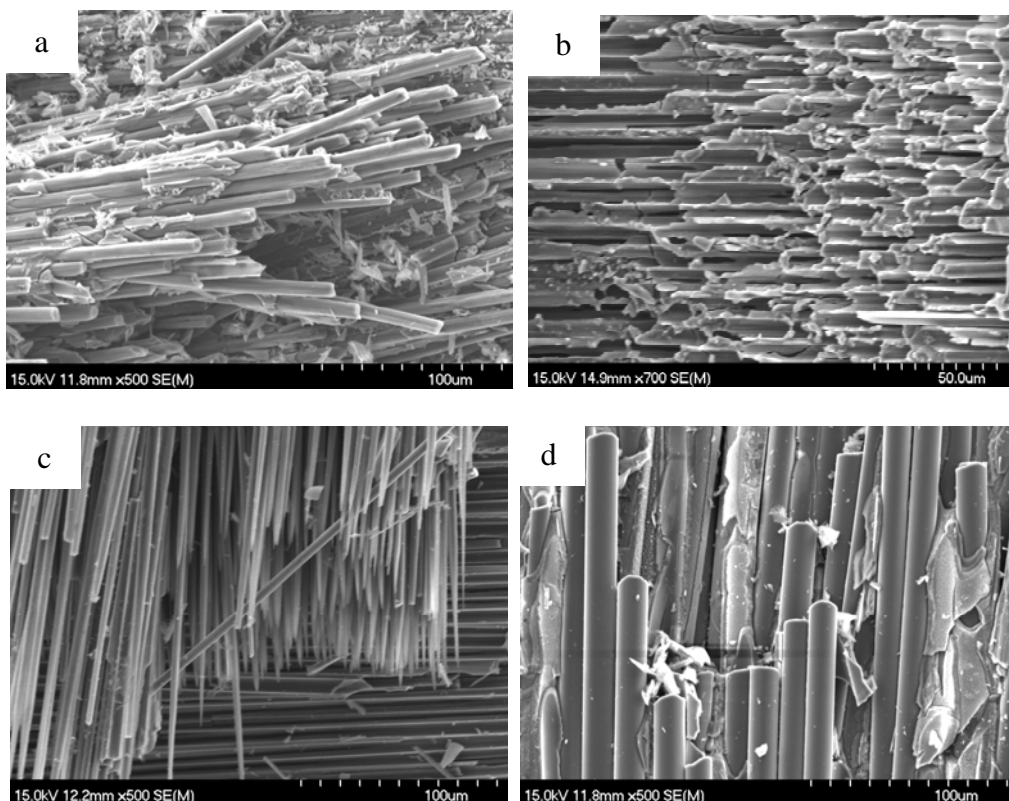
Figure 6. SEM images of 2.5D-C/SiC at fracture surface (a) and near notch (b),
2D-C/SiC (c) and 2D-SiC/SiC (d) failed by interlaminar shear load

4. Conclusions

(1)At 1173K in air, ILSS of 2D-C/SiC is higher than that of 2.5D-C/SiC along the warp direction，but considerably lower compared with that of the weft direction for 2.5D-C/SiC. ILSS for 2D-SiC/SiC is considerably higher than that of 2D-C/SiC.

(2) The great shear anisotropy between the warp and weft direction for 2.5D-C/SiC is associated with the characteristics of fiber preform architectures. For 2D-SiC/SiC and 2D-C/SiC composites, the difference of ILSS is mainly attributed to the kinds of fiber and oxidation of carbon fibers in the latter at 1173K in air.

References

[1] R.R. Naslain, António Pereira Nascimento Filho, Processing of ceramic matrix composites. Key Eng Mater, 164–165(1998) 3-8.

[2] K.G. Dassios, D.G. Aggelis, E.Z. Kordatos, T.E. Matikas, Cyclic Loading of a SiC-fiber Reinforced Ceramic Matrix Composite Reveals Damage Mechanisms and Thermal Residual Stress State. Composites Part A: Applied Science and Manufacturing, 44(2013) 105-113.

[3] L. Daniel and G. Ramusat, ''Prospective and Economic Impact of Composites in Reusable Launch Vehicle,'' AIAA, 2005-6618.

[4] Yan KF, Zhang CY, Qiao SR, Li M, Han D, Failure and strength of 2D-C/SiC composite under in-plane shear loading at elevated temperatures. Mater Des, 32(2011) 3504–8.

[5] Camus G, Guillaumat L, Baste S, Development of damage in a 2D woven C/SiC composite under mechanical loading. Compos Sci Technol, 56(1996) 1363-72.

[6] Dalmaz A, Reynaud P, Rouby D, Fantozzi G, Abbe F, Mechanical behavior and damage development during cyclic fatigue at high-temperature of a 2.5D carbon/SiC composite. Compos Sci Technol, 58(1998) 693–9.

[7] Ö. Ünal, Narottam P, Bansal, In-plane and interlaminar shear strength of a unidirectional Hi-Nicalon fiber-reinforced celsian matrix composite. Ceramics International, 28(2002) 527–540.

[8] Choi SR, Bansal NP, Interlaminar tension/shear properties and stress rupture in shear of various continuous fiber-reinforced ceramic matrix composites. Ceram Trans, 175(2006) 119-34.

[9] Choi SR, Bansal NP, Shear strength as a function of test rate for SiC_f/BSAS ceramic matrix

composite at elevated temperature. J Am Ceram Soc, 87(2004) 1912–8.

[10] Sung R. Choia, Robert W. Kowalik, Donald J. Alexandera, Narottam P. Bansal, Elevated-temperature stress rupture in interlaminar shear of a Hi-Nic SiC/SiC ceramic matrix composite. Composites Science and Technology, 69(2009) 890-897.

[11] M.B. Ruggles-Wrenn, P.D. Laffey, Creep behavior in interlaminar shear of Nextel^{TM}720/alumina ceramic composite at elevated temperature in air and in steam. Composites Science and Technology, 68 (2008) 2260-6

[12] Wang HL, Zhang CY, Liu YS, Han D, Li M, Qiao SR, Temperature dependency of interlaminar shear strength of 2D-C/SiC composite. Mater Des, 36(2012) 172–176.

[13] ASTM Designation C-1425-05. Standard test method for interlaminar shear strength of 1-D and 2-D continuous fiber-reinforced advanced ceramics at ambient temperatures. ASTM Designation, 2005.

[14]Cheng LF, Xu YD, Zhang LT, Yin XW, Oxidation behavior of three dimensional C/SiC composites in air and combustion conditions [J]. Carbon, 38(2000) 2103-2108

[15] Franck Lamouroux and Gérald Camus, Kinetics and Mechanisms of Oxidation of 2D Woven C/SiC Composites: I, Experimental Approach. J. Am. Ceram. Soc, 77(1994) 2049-57.